https://doi.org/10.7735/ksmte.2019.28.4.210

J. Korean Soc. Manuf. Technol. Eng.
ISSN 2508-5107(Online)

Fabrication and Performance Tests of an Ultrasonic Cleaning System for Solar-cell Wafers

Hyunse Kim[a*], Euisu Lim[a], Yanglae Lee[a], Jong-Kweon Park[a]

태양전지 웨이퍼 용 초음파 세정 시스템 제작 및 성능실험

김현세[a*], 임의수[a], 이양래[a], 박종권[a]

[a] *Korea Institute of Machinery and Materials, 171, Jang-Dong, Yuseong-Gu, Daejeon 34103, Korea*

ARTICLE INFO

Article history:

Received	5	April	2019
Revised	11	June	2019
Accepted	5	August	2019

Keywords:
Ultrasonic
Wave
Finite element method (FEM)
Cleaning
Solar-cell wafer

ABSTRACT

In this study, a midsonic cleaning system for solar-cell wafers with a frequency of 750 kHz was designed and fabricated. Finite element analysis was used to design the system. The obtained peak admittance value was 750.0 kHz. Reflecting the analysis results, the system was fabricated and its admittance characteristic was measured. The measured data showed 753.1 kHz, a value that was consistent with the finite element method (FEM) result with 0.4% error. The acoustic pressure test was performed and the resulting pressures were found to range from 283% to 328%, with a standard deviations range from 36.8% to 39.2%. Then, the wafer damage test was performed, and no damage was observed. Finally, the particle-cleaning test was performed; when we applied 1100 W, 99.8% of particles were removed. These results indicate that the developed midsonic bath has the capability of cleaning effectively without inflicting wafer breakage.

1. Introduction

Ultrasound has been widely applied in a variety of industries, such as in manufacturing, industrial cleaning and semiconductor wafer cleaning processes[1-12]. Regarding manufacturing fields, Luo et al. and Jang et al. reported ultrasonic bonding process, and Ng et al. explained ultrasonic welding application[1-3]. In addition, it can be used for micro hole machining, hot embossing, burnishing polishing and nano-surface reformation process[4-8]. In our previous works, ultrasonic waveguides for semiconductor wafer cleaning apparatus are included[11,12]. Some researches are reported about megasonic cleaning mechanisms[13,14].

In this research, we have used ultrasound for a solar-cell wafer cleaning system. Recently, solar energy has attracted attention as a promising clean energy source in the future, and solar energy generating systems are being widely developed. The major energy converting photovoltaic parts are fabricated on solar cell wafers, and as a result the demands on manufacturing solar cell wafers have been rapidly increasing.

Solar cell wafers are generally manufactured through the

* Corresponding author. Tel.: +82-42-868-7967
Fax: +82-42-868-7355

E-mail address: hkim@kimm.re.kr (Hyunse Kim).

following 10 steps: (1) Ingots are grown as a wafer material. (2) As their shapes are not cylindrical, the top and tail parts are cut to make each end even. (3) Solar wafers are rectangular, so they are then cut into a rectangular shape. (4) Their surfaces are ground, and (5) they are cut into basic units. (6) Next is the slicing process for obtaining separate wafers; in this process, a substantial amount of debris is generated, so the wafers are pre-cleaned using the ultrasonic cleaning system. (7) The cut wafers are separated, then (8) they go through a second cleaning. (9) In order to observe any defects, quality tests are conducted and (10) they are finally wrapped for sale. Among these steps, the cleaning process is crucial for maintaining a contamination-free wafer condition.

The detailed recipes for the cleaning process are as follows. In the pre-cleaning process, 28 kHz, 40 kHz, and 40 kHz ultrasonic cleaning processes are involved in a sequence. For the second and final cleaning, 40 kHz ultrasonic with full power up to 900 W is used. In this process, due to the wafer breakage problem, the use of 250 W power is recommended. The cleaning recipes are illustrated in Fig. 1.

The conventional solar cell wafer thickness is 200 μm. As the wafer technologies continue to be developed, thinner wafers down to 100 μm are predicted to be incorporated for lowering manufacturing costs. Consequently, the wafer breakage issues should be solved in the final cleaning process. Furthermore, the cleaning criteria require less than

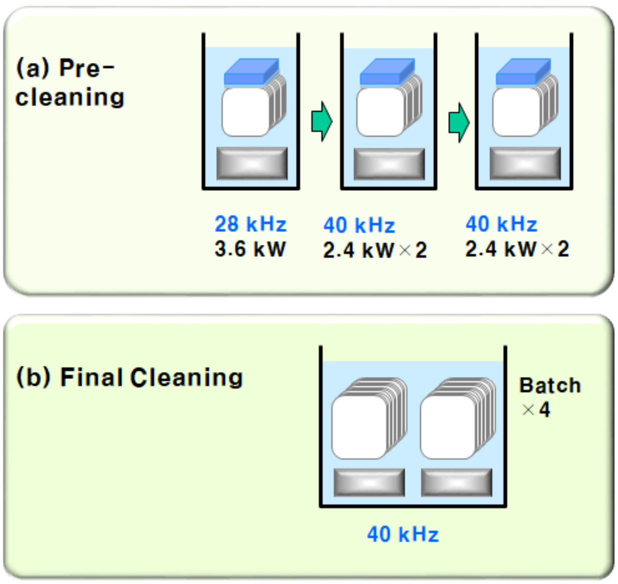

Fig. 1 Solar cell wafer cleaning processes

5 μm water mark or particles.

In this article, a midsonic cleaning system with a frequency of 750 kHz in the midsonic range between 100 kHz and 1 MHz is designed and fabricated. Finite element analysis was used to design the actuator and the stainless steel plate. Then, performance tests are processed in the point of acoustic pressure output and the wafer cleaning efficiency with the breakage test. Finally, the results are compared with those of a conventional type, and the performance is discussed.

2. Fabrication of an Ultrasonic System

2.1 System Configuration

For solar cell wafer cleaning, the conventional ultrasonic frequencies are 28 kHz and 40 kHz. We will use the midsonic range, which refers to the range between 100 kHz and 1 MHz. We set the design frequency at 750 kHz, which is in the upper middle of the midsonic range, and much higher than those set in previously described technologies. The reason of choosing the 750 kHz frequency is for shortening the propagating wavelength to lower the wafer damage possibility. When we consider the basic equation,

$$V = f \cdot \lambda \tag{1}$$

where v is the velocity of sound, f is the frequency, and λ is the wavelength, a lower frequency means bigger λ, while a higher frequency involves smaller λ. As a result, the chance of damage occurring can be substantially reduced by incorporating a higher frequency. In other words, λ is reduced by approximately 1/40 times for 750 kHz operation, as compared to 28 kHz. In addition, the removable particle size range of the conventional ultrasonic system is between 100 μm and 1 mm, but in the midsonic system, particles between 1 μm and 100 μm can be cleaned[10].

Furthermore, we adapted far-field wave, which differs from the general near-field type. The difference in the working principle is illustrated in Fig. 2. As shown in the figure, the near-field type uses a relatively thinner resonance plate, so the acoustic pressure distribution is irregular at the working distance. By contrast, the far-field type incorporates a thicker resonance plate, and as a result, the acoustic pressure distribution is more uniform than the latter. Similarly, there

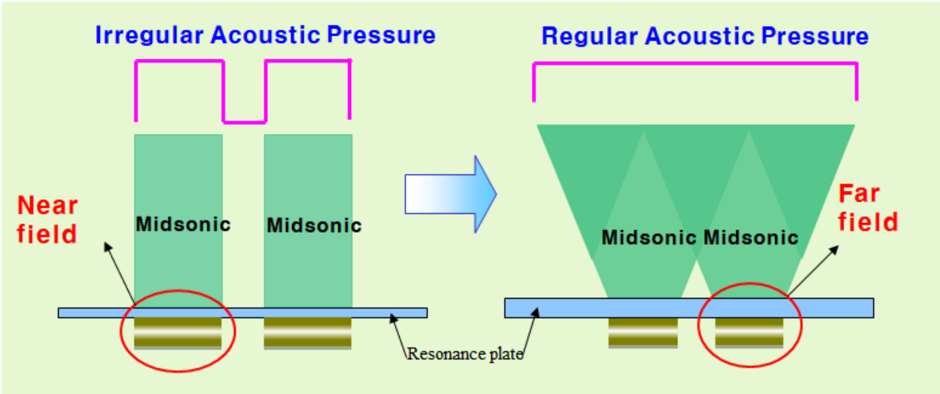

(a) (b)

Fig. 2 Difference in the working principle between (a) near-field wave and (b) far-field

are low odds of pattern damage. For the cleaning bath, there will be several rectangular piezoelectric ceramic actuators at the bottom. In the next chapter, we will describe the finite element method (FEM) process for the design of the plate.

2.2 Design and Fabrication of the Ultrasonic System

To design the ultrasonic system, finite element analysis was performed using commercial FEM tool ANSYS software. First, in order to design the actuator, it was modelled two-dimensionally as an axis-symmetric rectangular shape. The material of the actuator was piezoelectric ceramic, and the properties were given to the model. For actuation, electricity should be supplied, the top line and the bottom line were used as electrodes for the analysis. They were electrically coupled to each other, and 1 V was applied to the top while 0 V was applied to the bottom line as a ground. The calculations were done by changing the frequencies from 600.0 kHz to 900.0 kHz. The obtained admittance graph is shown in Fig. 3(a), and the peak admittance value was 750.0 kHz. Based on the analysis dimensions, a real piezoelectric ceramic actuator was fabricated, and the top and bottom surfaces were coated as electrodes. In order to make it easier to connect wires, the bottom electrode was drawn to the left lower corner of the top electrode. Subsequently, the admittance characteristic of the piezoelectric ceramic actuator was measured and plotted in Fig. 3(b). The peak value was 749.0 kHz, which was consistent with the previous analysis value. Thus, the value of 750.0 kHz was chosen as the design frequency of the system. The fabricated piezoelectric ceramic

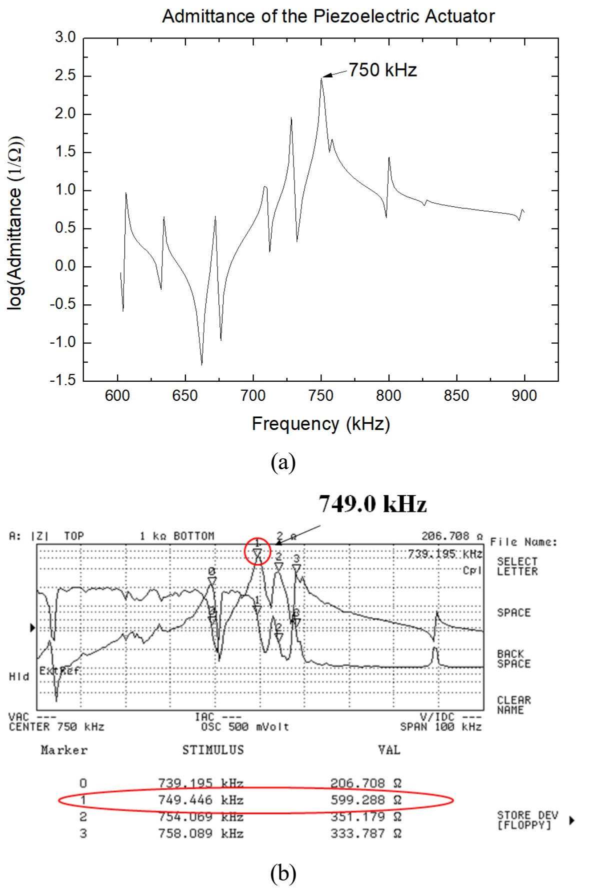

Fig. 3 (a) FEM admittance analysis result and (b) experimental result of the piezoelectric ceramic actuator

actuator (137 × 39 × 3 mm, a thin rectangular type) is shown in Fig. 4.

Secondly, the stainless steel plate with the piezoelectric ceramic actuator was also modelled two-dimensionally and axis-symmetrically. In the analysis, the top nodes and the

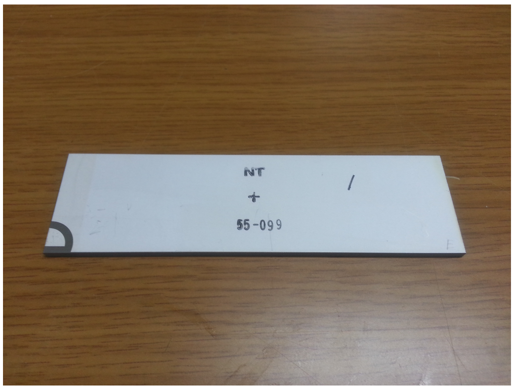

Fig. 4 Fabricated piezoelectric ceramic actuator

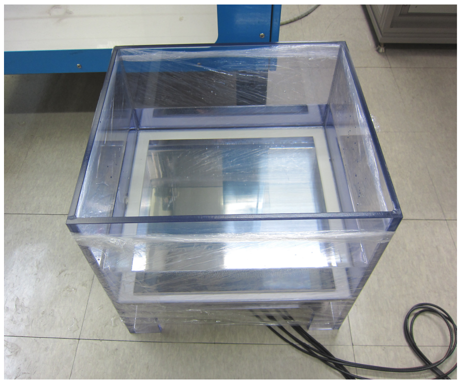

Fig. 6 Fabricated solar cell wafer cleaning bath

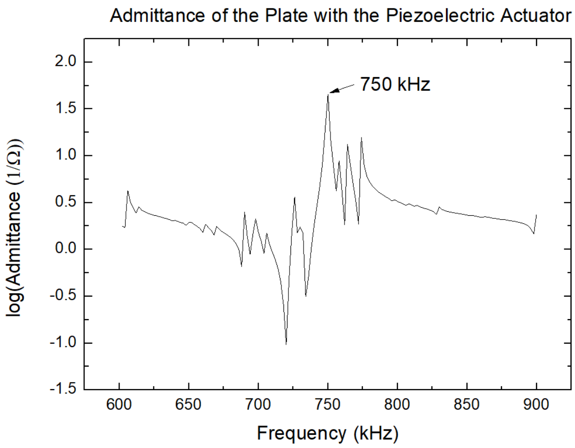

(a)

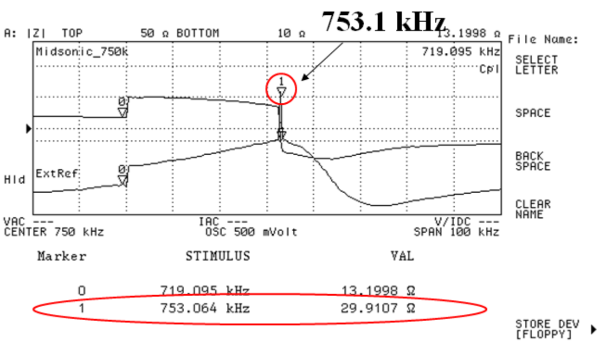

(b)

Fig. 5 (a) FEM admittance analysis result and (b) experimental result of the stainless steel plate with the piezoelectric ceramic actuator

bottom nodes were coupled as electrodes, and again, 1 V was applied to the top while 0 V was applied to the bottom line as a ground. The calculations were done between the same frequency ranges from 600.0 kHz to 900.0 kHz. The obtained peak admittance value was also 750.0 kHz, which was consistent with the measured data of 753.1 kHz, as shown in Figs. 5(a) and (b). Reflecting the analysis results, an stainless steel plate with eight piezoelectric ceramic actuators was fabricated, and the bath is shown in Fig. 6.

3. Experiments

3.1 Acoustic Pressure Measurement

After fabricating the ultrasonic bath, the acoustic pressure distributions were measured over the plate filled with water. The experimental setup is composed of a hydrophone sensor (Ø 2.5 × 70.0 mm, Onda corp.) attached on the jig, three-axis moving columns and a computer analysis system, as shown in Fig. 7. When measuring the data, the sensor is moving in a zig-zag path with 0.05 mm steps so that it can scan the desired area in detail. The measured data is transported to the computer and the pressure distributions are displayed in real time. After saving the data file, it is analyzed by calculating the maximum values and standard deviation values.

First, we filled the tank with water and started the power supply by regulating the electrical generator. The powers were increased from 200 W through 700 W, the values of which may not damage the solar wafers. When supplying power, the sensor will be immersed just below the surface of the water by 3 mm due to the object of the system, which is ensuring that it will work in the water for cleaning. We began measuring from the corner of the rectangular surface area and proceeded slowly to the other corner step by step to scan the acoustic pressures. The same procedures were repeated for increased powers, and three sets of tests were completed. The measured acoustic pressure distributions at 500 W power are shown in Fig. 8. The red tone bright area

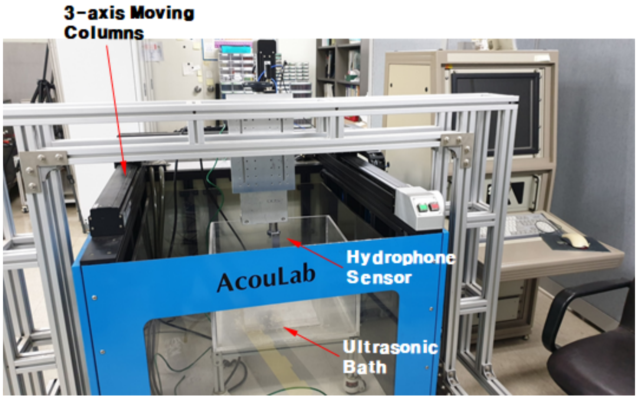

Fig. 7 Experimental setup

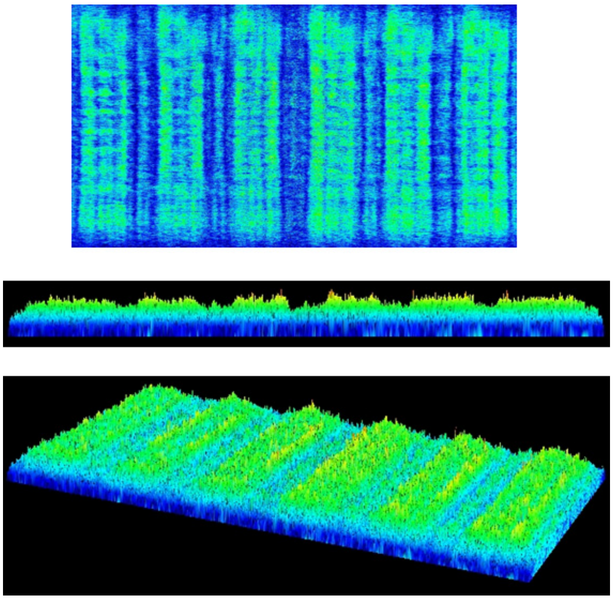

Fig. 8 Acoustic pressure distributions

means high acoustic pressures while the blue tone dark area indicates low acoustic pressure. Relatively uniform acoustic pressure distributions can be observed, which indicates a lower possibility of wafer damage.

For each data, the maximum values and standard deviation values were calculated. As a result, the maximum acoustic pressures over averaged values were found to range from 283% to 328%, and the standard deviations over averaged values were found to range from 36.8% to 39.2%. The results are plotted in Figs. 9(a) and (b).

3.2 Wafer Cleaning Test

At this time, in order to assess the system, the wafer cleaning test was processed. First, the wafer breakage test was processed. Two wafer sets were cleaned by a conventional

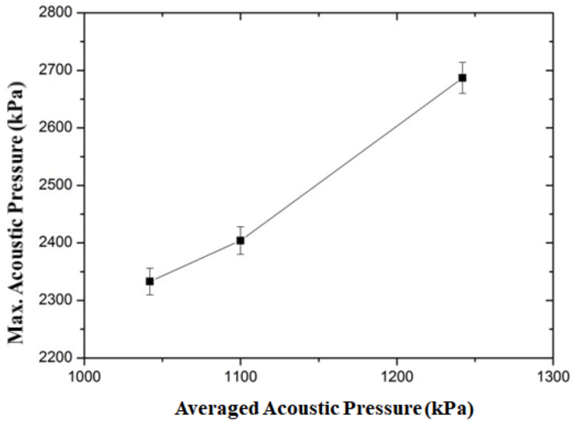

(a)

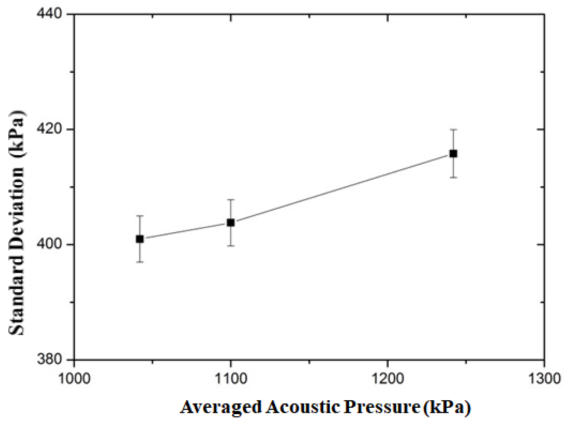

(b)

Fig. 9 Measured data: (a) maximum values and (b) standard deviation values

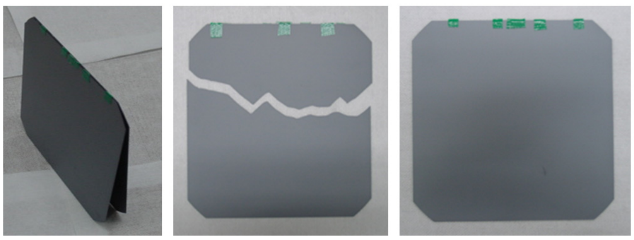

(a) (b) (c)

Fig. 10 (a) Test wafers and the results from (b) the 40 kHz bath and (c) the developed 750 kHz bath

40 kHz bath and the developed 750 kHz bath. The test wafers are shown in Fig. 10(a). The test bed includes an electric controller for the 40 kHz and 750 kHz baths. In the upper middle part, a cleaning liquid circulation tank is installed. Finally, the right-hand side contains cleaning test baths.

When the test wafer was submerged in the 40 kHz bath and cleaned, there was an instance of breakage over the wafer, as shown in Fig. 10(b). By contrast, when using the

Fig. 11 Particle counting test setup

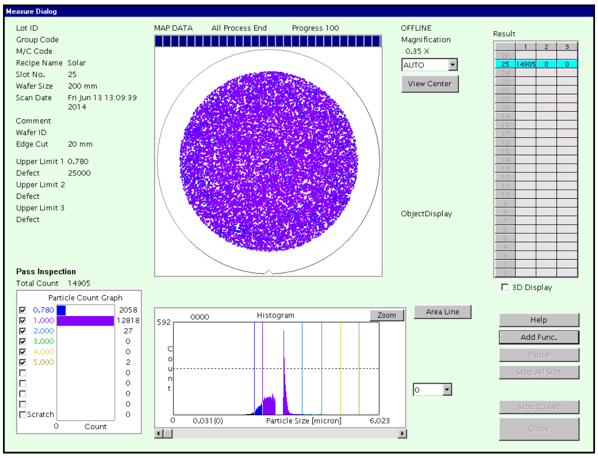

(a)

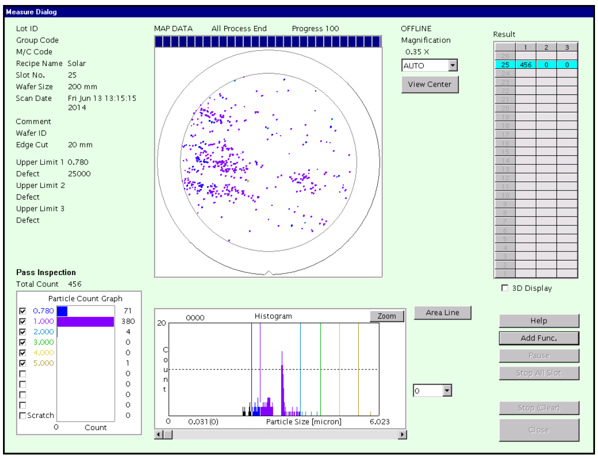

(b)

Fig. 12 Particle cleaning test results at 1000 W: (a) before and (b) after cleaning

developed 750 kHz bath, no damage over the wafer was observed, as shown in Fig. 10(c).

Finally, the particle cleaning test was processed. 1 μm-sized silica particles were deposited on 6-inch silicon (Si) wafers before test. Then, wafers before cleaning were analyzed with the particle counting machine (Topcon Corp.) as shown in Fig. 11. Then, they were cleaned by the 750 kHz bath for 90 seconds with different powers ranging from 0 W to 1000 W.

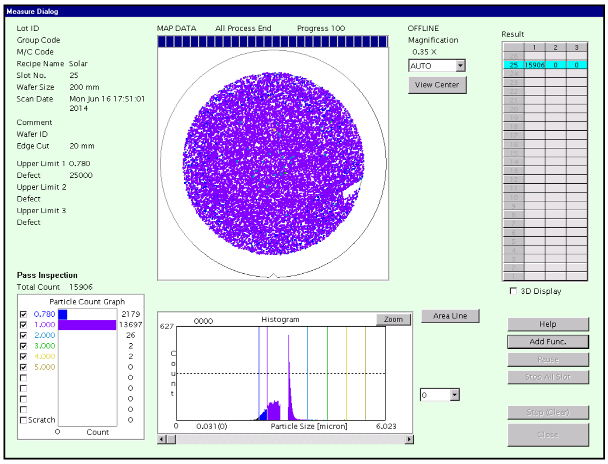

(a)

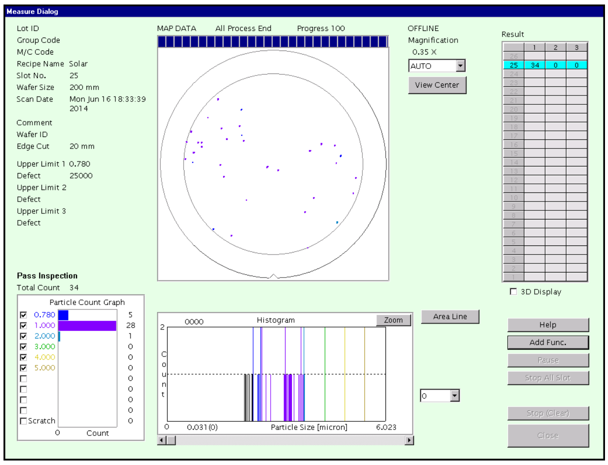

(b)

Fig. 13 Particle cleaning test results at 1100 W: (a) before and (b) after cleaning

Five wafers were tested for six different conditions. When we applied 1000 W, 97.0% of the particles were removed, as shown in Figs. 12(a) and (b), where before cleaning there were 14,905 particles and after there were 456 particles. Moreover, when we applied 1100 W, 99.8% of the particles were removed, as shown in Figs. 13(a) and (b), where before cleaning there were 15,906 particles and after there were 34 particles. The overall test results are plotted in Fig. 14. These results indicate that the developed 750 kHz bath has the capability to clean effectively without wafer breakage.

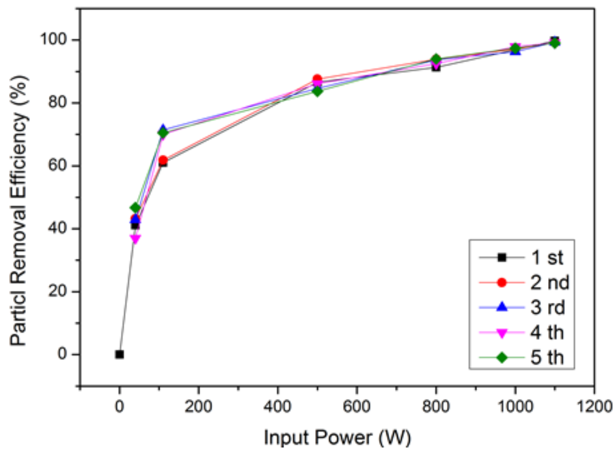

Fig. 14 Particle cleaning test results

4. Conclusion

In this work, a midsonic cleaning system with a frequency of 750 kHz in the midsonic range between 100 kHz and 1 MHz, was designed and fabricated. Finite element analysis was used for the design of the actuator and the stainless steel plate. The obtained peak admittance value was 750.0 kHz. Reflecting the analysis results, an stainless steel plate with eight piezoelectric ceramic actuators was fabricated with the bath and the admittance characteristic was measured. The measured data showed 753.1 kHz, which agreed well with the FEM result with 0.4% error.

Then, performance tests were processed in the point of acoustic pressure output and the wafer cleaning efficiency with the breakage test. For the acoustic pressure test, the maximum values and standard deviation values were measured and calculated. As a result, the maximum acoustic pressures were found to range from 283% to 328%, and the standard deviations were found to range from 36.8% to 39.2%. In addition, relatively uniform acoustic pressure distributions could be observed, which means a lower possibility of wafer damage.

Secondly, the wafer damage test was processed with the 40 kHz bath and the developed midsonic bath. The result showed that no damage over the wafer was observed with our midsonic bath.

Finally, the particle cleaning test was processed. When we applied 1000 W, 97.0% of the particles were removed, where before cleaning there were 14,905 particles and after there were 456 particles. Moreover, when we applied 1100 W, 99.8% of the particles were removed, where before cleaning there were 15,906 particles and after there were 34 particles.

These results explain that the developed 750 kHz bath has the capability to clean effectively without wafer breakage.

Acknowledgment

This research was supported by the Technology and Information Promotion Agency (TIPA), under the Korea government Ministry of Small and Medium-sized Enterprises (SMEs) and Startups. Additionally, it was also supported by the Fundamental Research Project (NK219B) of the Energy Systems Research Division at the Korea Institute of Machinery and Materials.

References

[1] Luo, Y., Zhang, Z., Wang, X., Zheng, Y., 2010, Ultrasonic Bonding for Thermoplastic Microfluidic Devices without Energy Director, Microelectronic Engineering, 87 2429-2436.

[2] Jang, H. S., Park, W. Y., Park, D. S., 2011, The Establishment of Bonding Conditions of Cu using an Ultrasonic Metal Welder, Journal of The Korean Society of Manufacturing Technology Engineers, 20:5 570-575.

[3] Ng, S. H., Wang, Z. F., Rooij, N. F. de, 2009, Microfluidic Connectors by Ultrasonic Welding, Microelectronic Engineering, 86:4-6 1354-1357.

[4] Park, S. J., Lee, B.-G., Choi, H.-Z., 2004, Micro hole Machining for Ceramics (Al_2O_3) using Ultrasonic Vibration, Journal of The Korean Society of Manufacturing Technology Engineers, 13:2 104-111.

[5] Mekaru, H., Goto, H., Takahashi, M., 2007, Development of Ultrasonic Micro Hot Embossing Technology, Microelectronic Engineering, 84:5-8 1282-1287.

[6] Li, F. L., Xia, W., Zhou, Z. Y., Zhao, J., Tang, Z. Q., 2012, Analytical Prediction and Experimental Verification of Surface Roughness during the Burnishing Process, International Journal of Machine Tools and Manufacture, 62 67-75.

[7] Zhao, Q., Sun, Z., Guo, B., 2016, Material Removal Mechanism in Ultrasonic Vibration assisted Polishing of Micro Cylindrical

Surface on SiC, International Journal of Machine Tools and Manufacture, 103 28-39.

[8] Kim, H., Lim, E., Park, J.-K., 2017, Development of a 20 kHz Ultrasonic System for Nano-surface Reformation Process, Journal of The Korean Society of Manufacturing Technology Engineers, 26:4 365-370, https://doi.org/10.7735/ksmte.2017.26.4.365.

[9] Geng, H., 2005, Semiconductor Manufacturing Handbook McGraw-Hill, New York.

[10] Kanegsberg, B., 2001, Critical Cleaning, CRC Press, Boca Raton, FL.

[11] Kim, H., Lee, Y., Lim, E., 2009, Design and Fabrication of an L-type Waveguide Megasonic System for Cleaning of Nano-scale Patterns, Current Applied Physics, 9 e189-e192.

[12] Kim, H., Lee, Y., Lim, E., 2013, Design and Fabrication of a Horn-type Megasonic Waveguide for Nanoparticle Cleaning, IEEE Transactions on Semiconductor Manufacturing, 26 221-225.

[13] Hauptmann, M., Struyf, H., Mertens, P., Heyns, M., De Gendt, S., Glorieux, C., Brems, S., 2013, Towards an Understanding and Control of Cavitation Activity in 1 MHz Ultrasound Fields, Ultrasonics Sonochemistry 20:1 77-88.

[14] Keswani, M., Raghavan, S., Deymier, P., 2013, Characterization of Transient Cavitation in Gas Sparged Solutions exposed to Megasonic Field using Cyclic Voltammetry, Microelectronic Engineering, 102 91-97.